J|A|C|S COMMUNICATIONS

Published on Web 02/01/2010

Synthesis of Supported Platinum Nanoparticles from Li−Pt Solid Solution

Tao Xu,*,† Chikai Lin,† Chao Wang,‡ Dale L. Brewe,§ Yasuo Ito,⊥ and Jun Lu⊥

Department of Chemistry and Biochemistry, Northern Illinois University, DeKalb, Illinois 60115, Materials Science Division, Argonne National Laboratory, Argonne, Illinois 60439, Advance Photon Source, Argonne National Laboratory, Argonne, Illinois 60439, Department of Physics, Northern Illinois University, DeKalb, Illinois 60115

Received November 13, 2009; E-mail: txu@niu.edu

Platinum nanoparticle catalysts are essential for achieving energy-efficient and greener chemical processes that involve breaking or establishing of H−H, C−H, or O−H bonds.[1] For example, Pt nanoparticles exhibit excellent catalytic activity in oxidative dehydrogenation reactions.[2] Carbon-supported Pt nanoparticles are among the most feasible catalysts for oxygen reduction reaction in fuel cells.[3]

To prepare such Pt nanoparticles, nearly all synthetic methods followed a bottom-up strategy, that is, Pt precursory molecules (precatalysts) are first reduced into Pt atoms, which then grow into polyatomic particles.[4] In contrast, the counter-strategy in nanomaterials synthesis, namely a top-down strategy, has been largely overlooked for preparation of Pt nanoparticles. In this report, we demonstrate an innovative top-down method to prepare the supported Pt nanoparticles (<2 nm), starting directly from bulk metallic Pt to bypass many complications in the synthesis methods using Pt precursors.[5] Consequently, our method can avoid chloride contamination, which will likely cause the loss of catalytic activity.[6] Furthermore, our method involves no stabilizing agents, which otherwise need to be removed in the solution-based bottom-up strategy to free the catalytic sites.[7] Finally, the Pt nanoparticles can be transferred to any nonaqueous solid support to avoid the harsh pretreatment of the support materials,[8] or the trapping of Pt catalysts in the deep cracks of solid support materials.[9]

As depicted in Scheme 1, liquid lithium was used as a solvent to dissolve bulk Pt into nanoscale nuclei at elevated temperature. A tip ultrasonic homogenizer was employed to facilitate the solvation of Pt in Li. The liquid 0.99Li−0.01Pt alloy (equivalent to 22 wt % Pt) was then quenched into a solid solution. Figure 1a and b showed Pt mapping image by an energy dispersive X-ray (EDX) detector and its corresponding EDAX analysis. The results suggest a microscopic homogeneity of Pt content in the Li−Pt alloy. Next, Li in the Li−Pt solid solution was converted into LiOH powder via a controlled gas−solid reaction $2Li\ (s) + 2H_2O\ (g) \rightarrow 2LiOH\ (s) + H_2\ (g)$ at 100 °C, which prevents the aggregation of the as-formed Pt nanoparticles. However, it should be noted that the safe handling of Li is required due to the reactivity of lithium.

Extended X-ray absorption fine structure (EXAFS) spectroscopy was used to determine the local atomic structure around Pt atoms and to evaluate Pt particle size in LiOH at a macroscopic level. The EXAFS spectra of Pt in LiOH and bulk Pt foil are shown in Figure 2a.

Figure 2b shows the corresponding Fourier transformed (FT) spectra. Essentially all the features of the bulk metallic Pt foil are reproduced by the Pt−LiOH mixture in the EXAFS and FT spectra, which indicates that the Pt content in LiOH is in the metallic state.

Scheme 1. Top-Down Synthesis of Supported Pt Nanoparticles from the Li−Pt Solid Solution

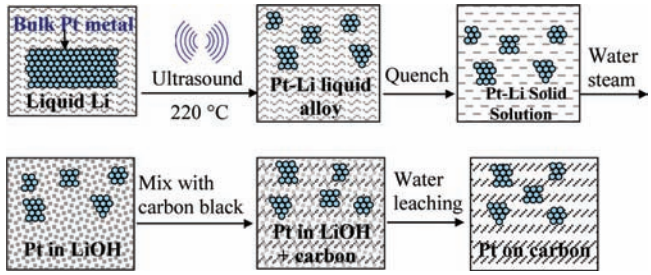

However, the peak intensities for Pt in LiOH are weaker than those of the bulk Pt foil. This implies a decrease in the average coordination numbers of Pt content embedded in Pt−LiOH, and therefore, strongly suggests the presence of Pt nanoparticles with a significant fraction of undercoordinated surface Pt atoms.[10] The EXAFS data was further analyzed using the Ifeffit package[11] as summarized in Table 1, assuming that the coordination number and Pt−Pt bond length for bulk Pt are 12 and 2.76 Å, respectively.[10]

To estimate the mean particle size using EXAFS, we employed the method described by Calvin *et. al*,[12] in which they assumed that the coordination numbers of spherical nanoparticles are reduced by a factor of $1-0.75(r/R) + 0.0625(r/R)^3$ relative to a bulk crystal, where R is the radius of the particle and r is the Pt−Pt bond length.[18] Using the near-neighbor (NN) distance and reduction in coordination number obtained from the EXAFS analysis (see Figure S4 in Supporting Information), the estimated diameter of our Pt nanoparticles in LiOH is ∼1.7 ± 0.2 nm. The bond-length disorder (i.e., σ^2) in the as-formed Pt nanoparticles by the top-down method is comparable to the bulk foil, ($|\sigma^2_{(particle)} - \sigma^2_{(bulk)}|/\sigma^2_{(bulk)} < 3\%$). We believe that the Pt nanoparticles prepared by the top-down method are just nanochips of the bulk Pt so that they inherit the disorder of bulk Pt .

The Pt in LiOH powder was then ground with untreated carbon black as an example to represent any water-insoluble support materials. The mixture was rinsed with copious amounts of water

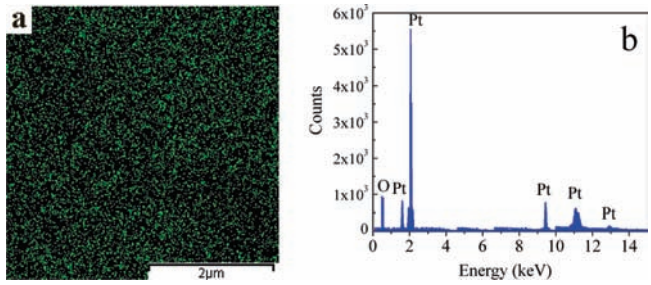

Figure 1. (a) Pt EDS mapping image of a freshly cut 0.99Li−0.01Pt solid solution and (b) its corresponding EDS profile.

† Department of Chemistry and Biochemistry, Northern Illinois University.
‡ Materials Science Division, Argonne National Laboratory.
§ Advance Photon Source, Argonne National Laboratory.
⊥ Department of Physics, Northern Illinois University.

10.1021/ja909442c

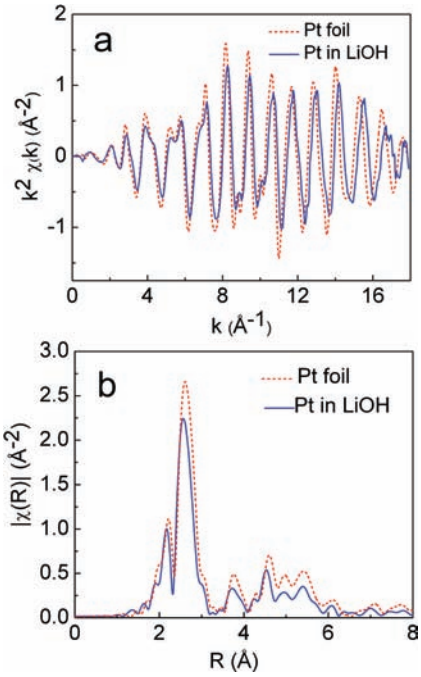

Figure 2. (a) The EXAFS spectra of Pt in LiOH and a Pt foil and (b) the EXAFS Fourier-transformed (FT) to *R*-space. The results suggest the average Pt particle size is 1.7 ± 0.2 nm.

Table 1. Parameters of Pt−LiOH and Pt Foil Obtained from EXAFS

parameters relative to theory	Pt in LiOH	Pt foil
NN coordination number relative to theory	0.76 ± 0.05	1.01 ± 0.03
bond length (Å)	2.730 ± 0.002	2.757 ± 0.001
bond length disorder σ^2 (Å^2)	0.0049 ± 0.0002	0.0052 ± 0.0001

under ambient condition to selectively leach off the LiOH, allowing Pt nanoparticles to be adsorbed on the neighboring carbon support.

The resulting carbon-supported Pt nanoparticles were characterized by scanning transmission electron microscopy and transmission electron microscopy (STEM/TEM). STEM high-angle annular dark-field (HAADF) image (Figure 3a) shows significantly brighter contrast on the particles against that of supporting media, indicating that these particles consist of the atoms with significantly higher atomic numbers.[13] EDS indicates only Pt and carbon are present (Figure S2, Supporting Information). Figure 3b shows a typical bright-field TEM image, which demonstrates that the particle size of the as-formed Pt nanoparticles is around 2 nm (dark spots), with a narrow size distribution as shown in Figure 3c (see also Figure S5, Supporting Information). This is in good agreement with EXAFS results for Pt nanoparticles in LiOH, indicating that the aggregation of Pt nanoparticles is minimized during the replacement of the support from LiOH to carbon black. This is important to maintain the high catalytic properties of the as-formed Pt nanoparticles.

According to the Li−Pt binary phase diagram (Figure S1, Supporting Information),[14] Li−Pt liquid alloy is obtained at temperature above 200 °C with Pt content of 1 at % (~22 wt %) in this study. To avoid any possible formation of intermetallic compounds during the cooling process, the Li−Pt liquid solution was rapidly solidified to form a metastable Li−Pt solid solution. Miyazaki et al. revealed that the critical minimum size of precipitate in the vicinity of the edge of the miscibility gap of a binary alloy is extremely sensitive to the alloy composition around the phase

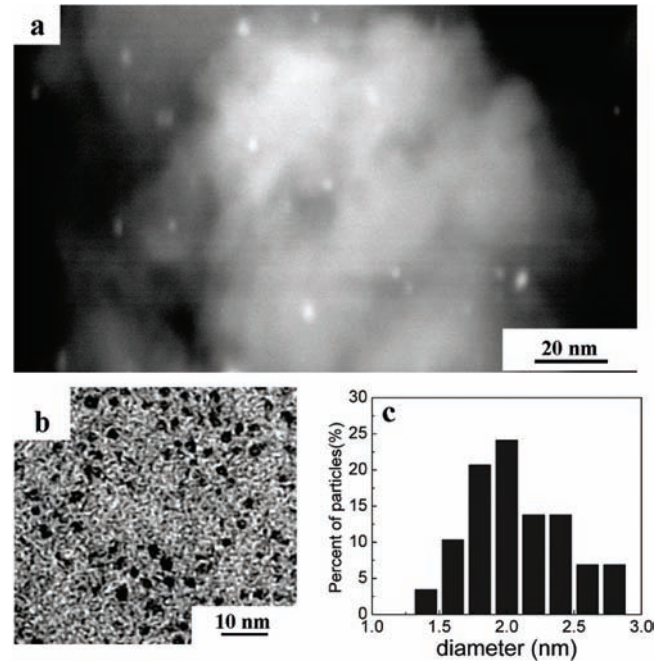

Figure 3. (a) Representative HAADF STEM image of Pt particles on carbon black. (b) Representative bright-field TEM image of Pt nanoparticles (15 wt %) on carbon black (c) Histogram of particle size diameters 1.9 ± 0.3 nm.

boundary.[15] Hence, the key to achieving small Pt nanoparticles is to set the Li−Pt composition away from the phase boundary. In our case, 1 at % Pt is far away from the phase boundary of Li_5Pt. The observation of Pt nanoparticles (<2 nm) from STEM/TEM and EXAFS analysis does support the presence of the very small Pt nuclei in the Li−Pt alloy. It should also be mentioned that the use of ultrasound efficiently facilitates the solvation and dispersion of the Pt nanoparticles in the liquid lithium solvent.

A primary electrocatalytic characterization for oxygen reduction reaction (ORR) was conducted to investigate the catalytic property of the carbon-supported Pt nanoparticles. The prepared Pt/C nanoparticles (with 15% Pt) were dispersed in water by sonication and the formed suspension was deposited on a glassy carbon electrode. The loading of Pt was controlled to be 15 $\mu g_{Pt}/cm^2$ disk. Typical hydrogen desorption/adsorption peaks at potentials <0.4 V (vs reversible hydrogen electrode, RHE) are observed in the cyclic voltammogram (CV), as shown in Figure 4a, based on which the electrochemical surface area was calculated to be 2.8 cm^2,[16] which was used to normalize the electrode current for specific activity. Figure 4b shows the specific activity based on the polarization curve measured by rotational disk electrode (RDE) (Figure S3, Supporting Information). At 0.9 V vs RHE, the catalytic activity of our Pt/C sample reached 0.53 mA/cm^2, which has a improvement factor close to three compared with the benchmark for commercial Pt/carbon catalyst in the literature.[3] The enhanced catalytic activity is likely due to the unique top-down synthetic approach which produces nanoparticles inheriting more characteristics of the bulk Pt material, which is well-known to possess higher specific activity than Pt nanoparticles.[17] In addition, the stability of the catalyst is comparable with commercial Pt/C catalysts with the same size. The diminishment of crystal defects in these nanoparticles could substantially enhance the durability of the catalyst against the nanoparticles prepared by bottom-up approaches of the same size. As an evidence, CV shown in Figure 4 was recorded at 100th cycle, and the voltammogram was stable with this number of cycles.

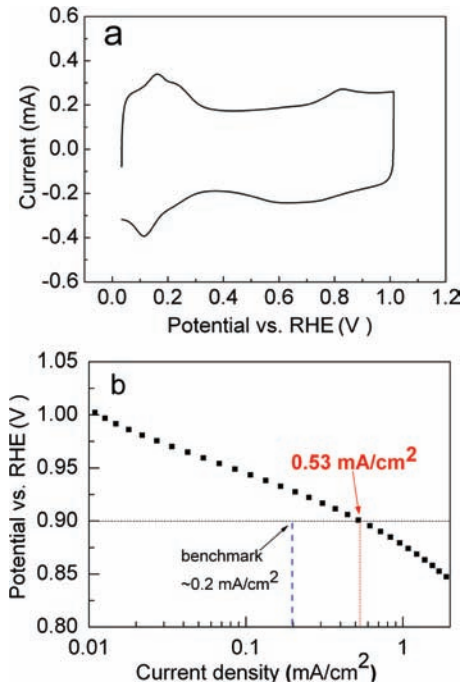

Figure 4. Electrocatalytic characterization of ultrasmall Pt/C prepared by the solid solution method, (a) cyclic voltammogram, and (b) specific activity. The benchmark shown in (b) is cited from ref 3.

Finally, it should be noted that Schrinner et al. recently reported the synthesis of Pt nanocrystals (2−4 nm) by partial dissolution of Au−Pt nanoalloys in lethal cyanide solutions.[18] Their method is fundamentally different from ours, since their starting material is Pt−Au nanoparticles prepared from the conventional precursory method. More importantly, our method used no toxic agents, and it is flexible in the choice of support materials and free of contaminants.

In summary, we have prepared Pt nanoparticles with size less than 2 nm through an unique top-down strategy using liquid Li as a solvent to break down bulk Pt. We previously showed that Pd can also be evenly dissolved in liquid Li.[19] Thus, this top-down strategy can potentially be used for syntheses of supported nanoparticles of other platinum group and noble metals, since Li forms liquid alloys with Pd, Ru, Rh, Ir, Au, Ag at relatively low temperatures.[20]

Acknowledgment. PNC/XOR facilities at the Advanced Photon Source and research at these facilities are supported by the U.S. Department of Energy - Basic Energy Sciences, a Major Resources Support Grant from NSERC, the University of Washington, Simon Fraser University, and the Advanced Photon Source. Use of the Advanced Photon Source is also supported by the U.S. Department of Energy, Office of Science, Office of Basic Energy Sciences, under Contract DE-AC02-06CH11357. The electron microscopy was accomplished at the Electron Microscopy Center for Materials Research at Argonne National Laboratory, a U.S. Department of Energy Office of Science Laboratory operated under Contract DE-AC02-06CH11357 by UChicago Argonne, LLC.

Supporting Information Available: Experimental details, Pt−Li phase diagram, EDS study on the Pt-carbon sample, more TEM images, polarization curve, details on EXAFS. This material is available free of charge via the Internet at http://pubs.acs.org.

References

(1) Gates, B. C. *Chem. Rev.* **1995**, *95*, 511.
(2) Vajda, S.; Pellin, M. J.; Greeley, J. P.; Marshall, C. L.; Curtiss, L. A.; Ballentine, G. A.; Elam, J. W.; Catillon-Mucherie, S.; Redfern, P. C.; Mehmood, F.; Zapol, P. *Nat. Mater.* **2009**, *8*, 213.
(3) (a) Gasteiger, H. A.; Kocha, S. S.; Sompalli, B.; Wagner, F. T. *Appl. Catal., B* **2005**, *56*, 9. (b) Zaragoza-Martín, F.; Sopeña-Escario, D.; Morallón, E.; Salinas-Martínez de Lecea, C. *J. Power Sources* **2007**, *171*, 302.
(4) (a) Xu, Z.; Xiao, F. S.; Purnell, S. K.; Alexeev, O.; Kawi, S.; Deutsch, S. E.; Gates, B. C. *Nature* **1994**, *372*, 346. (b) Ahmadi, T. S.; Wang, Z. L.; Green, T. C.; Henglein, A.; El-Sayed, M. A. *Science* **1996**, *272*, 1924.
(5) Kettler, P. B. *Org. Process Res.Dev.* **2003**, *7*, 342.
(6) (a) Zhao, X. S.; Sun, G. Q.; Jiang, L. H.; Chen, W. M.; Tang, S. H.; Zhou, B.; Xin, Q. *Electrochem. Solid-State Lett.* **2005**, *8*, A149. (b) Bönnemann, H.; Brinkmann, R.; Kinge, S.; Ely, T. O.; Armand, M. *Fuel Cells* **2004**, *4*, 289.
(7) (a) Salavagione, H. J.; Sanchis, C.; Morallon, E. *J. Phys. Chem. C* **2007**, *111*, 12454. (b) Wang, C.; van der Vliet, D.; Chang, K.; You, H.; Strmcnik, D.; Schlueter, J. A.; Markovic, N. M.; Stamenkovic, V. R. *J. Phys. Chem. C* **2009**, *113*, 19365.
(8) (a) Solar, J. M.; Leon, C. A. L.; Osseoasare, K.; Radovic, L. R. *Carbon* **1990**, *28*, 369. (b) Amine, K.; Mizuhata, M.; Oguro, K.; Takenaka, H. *J. Chem. Soc., Faraday Trans.* **1995**, *91*, 4451. (c) Coloma, F.; Sepulveda-Escribano, A.; Fierro, J. L. G.; Rodriguez-Reinoso, F. *Langmuir* **1994**, *10*, 750.
(9) (a) Matsumoto, T.; Komatsu, T.; Arai, K.; Yamazaki, T.; Kijima, M.; Shimizu, H.; Takasawa, Y.; Nakamura, J. *Chem. Commun.* **2004**, 840. (b) Thompson, S. D.; Jordan, L. R.; Forsyth, M. *Electrochim. Acta* **2001**, *46*, 1657.
(10) (a) Frenkel, A. I.; Hills, C. W.; Nuzzo, R. G. *J. Phys. Chem. B* **2001**, *105*, 12689. (b) Ramallo-Lopez, J. M.; Santori, G. F.; Giovanetti, L.; Casella, M. L.; Ferretti, O. A.; Requejo, F. G. *J. Phys. Chem. B* **2003**, *107*, 11441.
(11) (a) Newville, M. *J. Synchrotron Rad.* **2001**, *8*, 322. (b) Ravel, B.; Newville, M. *J. Synchrotron Rad.* **2005**, *12*, 537.
(12) Calvin, S.; Luo, S. X.; Caragianis-Broadbridge, C.; McGuinness, J. K.; Anderson, E.; Lehman, A.; Wee, K. H.; Morrison, S. A.; Kurihara, L. K. *Appl. Phys. Lett.* **2005**, *87*, 233102.
(13) (a) Jesson, D. E.; Pennycook, S. J. *Proc. R. Soc. London* **1995**, *449*, 273. (b) Menard, L. D.; Gao, S.-P.; Xu, H.; Twesten, R. D.; Harper, A. S.; Song, Y.; Wang, G.; Douglas, A. D.; Yang, J. C.; Frenkel, A. I.; Nuzzo, R. G.; Murray, R. W. *J. Phys. Chem. B* **2006**, *110*, 12874. (c) Kang, J. H.; Menard, L. D.; Nuzzo, R. G.; Frenkel, A. I. *J. Am. Chem. Soc.* **2006**, *128*, 12068.
(14) Sangster, J.; Pelton, A. D. *J. Phase Equilib.* **1991**, *12*, 678.
(15) Miyazaki, T.; Kobayashi, S.; Koyama, T. *Metall. Mater. Trans A* **1999**, *30*, 2783.
(16) Wang, C.; Daimon, H.; Lee, Y.; Kim, J.; Sun, S. *J. Am. Chem. Soc.* **2007**, *129*, 6974.
(17) Markovic, N. M.; Ross, P. N. *Surf. Sci. Rep.* **2002**, *45*, 121.
(18) Schrinner, M.; Ballauff, M.; Talmon, Y.; Kauffmann, Y.; Thun, J.; Moller, M.; Breu, J. *Science* **2009**, *323*, 617.
(19) Lin, C.; Xu, T.; Yu, J.; Ge, Q.; Xiao, Z. *J. Phys. Chem. C* **2009**, *113*, 8513.
(20) (a) Sangster, J.; Pelton, A. D. *J. Phase Equilib.* **1992**, *13*, 63. (b) Sangster, J.; Pelton, A. D. *J. Phase Equilib.* **1991**, *12*, 682. (c) Sangster, J.; Pelton, A. D. *J. Phase Equilib.* **1991**, *12*, 682. (d) Sangster, J.; Pelton, A. D. *J. Phase Equilib.* **1992**, *13*, 59. (e) Pelton, A. D. *J. Phase Equilib.* **1986**, *7*, 228. (f) Pelton, A. D. *J. Phase Equilib.* **1986**, *7*, 223.

JA909442C